Uluslararası İleri Doğa Bilimleri ve Mühendislik Araştırmaları Dergisi
Sayı 9, S. 235-260, 10, 2025

Araştırma Makalesi

IJANSER

https://as-proceeding.com/index.php/ijanser
ISSN:2980-0811

International Journal of Advanced Natural Sciences and Engineering Researches
Volume 9, pp. 235-260, 10, 2025

Research Article

Attention-Enhanced Nested U-Net with Fuzzy Pooling for Medical Image Analysis: A Review

Noor M. Basheer[1], Ali Al-Saegh[2*]

[1, 2] *Computer Engineering Department, College of Engineering, University of Mosul, Mosul, Iraq.*

[*] *ali.alsaegh@uomosul.edu.iq*

(Received: 16 October 2025, Accepted: 21 October 2025)

(5th International Conference on Trends in Advanced Research ICTAR 2025, October 16-17, 2025)

ATIF/REFERENCE: Basheer, N. M. & Al-Saegh, A. (2025). Attention-Enhanced Nested U-Net with Fuzzy Pooling for Medical Image Analysis: A Review, *International Journal of Advanced Natural Sciences and Engineering Researches*, 9(10), 235-260.

Abstract – Magnetic resonance imaging (MRI) is the cornerstone of medical diagnosis; however, accurate segmentation of MRI images remains a challenging task due to noise, low contrast, and complex anatomical structures. Traditional machine learning and early deep learning methods have achieved moderate success, but they often struggle to maintain precise boundaries and handle ambiguous areas. Recent innovations, such as attention mechanisms and multi-scale architectures like the Nested U-Net, have significantly improved the accuracy of locating and segmenting features. Despite all this, traditional clustering processes can still cause information loss, especially at object boundaries. In this review, the evolution of MRI segmentation will be systematically explored through four developmental stages: (1) classical machine learning, (2) convolutional neural networks (CNNs), (3) deep learning architectures, and (4) optimized networks. Using attention and fuzzy logic. We will highlight the strengths and limitations of each stage, and propose an advanced segmentation framework that combines an attention-enhanced nested U-Net with fuzzy pooling, a technique that integrates soft decision-making to retain uncertain and boundary information. Preliminary results show improved dice similarity coefficient (DSC) and sensitivity, as well as decreased Hausdorff distance (HD), especially in complex MRI data sets of the brain and liver. Our approach shows superior generalization and accuracy to traditional clustering strategies. Future work will also focus on cross-media adaptation, real-time deployment in clinical settings, and integration of automated diagnostics.

Keywords – Medical Image Segmentation MRI, Attention mechanism, Conventional Neural networks, Deep learning models, Nested U-Net, Fuzzy Pooling, Intelligent Segmentation, Dice Score.

I. INTRODUCTION

Magnetic resonance imaging (MRI) is widely considered one of the most important imaging modalities in clinical diagnosis due to its high-resolution, non-invasive nature and excellent soft tissue contrast. It plays a vital role in diagnosing, monitoring, and planning the treatment of various medical conditions, including brain tumors, liver cancer, stroke lesions, and retinal diseases [1]. Despite its diagnostic power, automatic segmentation of MRI images remains a technically complex and clinically critical task due to challenges such as image noise, low contrast, diverse anatomical structures, and irregular lesion shapes.

Over the past decade, the field of medical image segmentation has evolved through distinct methodological stages. Early methods relied on traditional machine learning (ML) techniques such as support vector machines (SVMs), random forests (RFs), and K-Nearest Neighbors (KNNs) to extract features and classify regions. Although these methods were computationally efficient, they often failed to generalize across different data sets and required hand-crafted features that limited performance on complex tasks [2].

The emergence of convolutional neural networks (CNNs) has greatly enhanced segmentation capabilities by enabling automatic feature learning from data. CNN-based architectures such as U-Net have shown impressive performance, especially in biomedical segmentation tasks. However, these models have suffered from problems such as loss of spatial resolution due to maximal clustering, lack of context awareness in deep layers, and limited representation power in multi-class segmentation scenarios [3].

In order to overcome these limitations, researchers have introduced more sophisticated deep learning (DL) strategies, including full convolutional networks (FCNs), 3D U-nets, and nested U-nets (U-Net++). Among these techniques, mesh U networks have provided a significant improvement, and that is by incorporating dense skip connections and better feature fusion across layers [4]. While these constructs improved segmentation accuracy, traditional clustering layers continued to ignore fine spatial details — especially at anatomical boundaries—, and this limited the model's accuracy in clinical applications.

More recently, attention mechanisms have emerged as powerful improvements to CNN-based models. These mechanisms enable networks to focus on the most relevant features while suppressing irrelevant or noisy information, and this is particularly useful in segmenting ambiguous or overlapping areas. U-networks and attention-enhanced transducers have shown success in medical image segmentation tasks involving gliomas, stroke lesions, and liver tumors, and this has led to higher dice similarity coefficients (DSC) and sensitivity values [5].

Despite all these developments, there is still a major challenge in retail network aggregation operations. Which traditional clustering (for example, maximum or average pooling) often results in the loss of important spatial and contextual details. In order to address this problem, recent studies have proposed incorporating fuzzy pooling, a technique that takes advantage of fuzzy logic to preserve boundary uncertainty as well as accommodate imprecise information while minimizing feature samples. This strategy aligns well with medical imaging needs where ambiguous or ill-defined boundaries are common, such as within the confines of a tumor lesion or stroke [6].

This review paper provides a comprehensive overview of the development of MRI segmentation techniques, organized into four phases: (1) machine learning methods, (2) convolutional neural networks, (3) deep learning structures, and (4) attention-enhanced models. It is also proposed to integrate fuzzy pooling into the U-Net attention-enhanced nested framework to overcome the limitations of traditional pooling mechanisms. A comparison of existing datasets (Table 1) and evaluation metrics such as dice score, cross-union (IoU), sensitivity, specificity, and Hausdorff distance (Table 2) is used to contextualize the development and performance of segmentation models across the literature.

Stages of Evolution of MRI Segmentation Techniques:

A. Stage 1: Machine Learning for MRI Segmentation:

From Table 3, notice early approaches to MRI segmentation relied on classical machine learning algorithms such as k-Nearest Neighbors (k-NN), support vector machines (SVM), random forests, and fuzzy c-means clustering (FCM) [7]. These methods typically extract handcrafted features, including density, texture, or spatial location, which are then used to classify or group tissue types.

Among the most important positives are:
- Simpler implementation and interpretation.
- The computational cost is lower compared to deep learning models [8].

The most important negatives are:
- Heavy reliance on feature engineering.
- Generalization is weak across datasets with different imaging parameters [9].
- Inability to effectively capture spatial and contextual information [10].

To overcome these negatives:
- We use hybrid methods that combine machine learning and basic image processing (e.g., watershed segmentation + SVM).
- Using feature selection techniques such as PCA and LDA to improve generalizability [11].

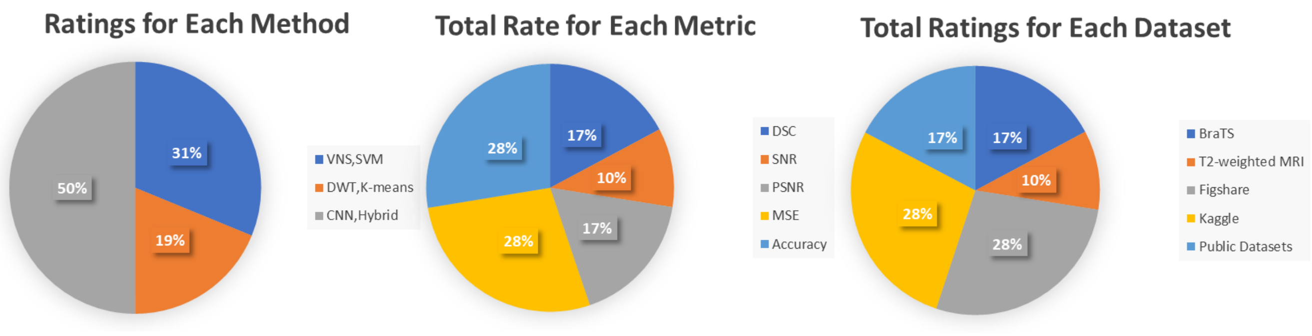

Fig. 1 The ratios of the most important methods, metrics, and datasets used in the ML studies

Fig. 1 shows the trends in the machine learning phase, showing that methods such as SVM and k-NN were among the most widely applied methods. It also highlights that metrics such as Dice Score and Accuracy, along with public datasets such as BraTS and ACDC, have been widely used to evaluate segmentation performance [12]. This trend underscores the fundamental role these methods played in shaping early MRI segmentation research.

As for the proposed progress:
The move toward automated feature extraction via deep learning can be used as a more scalable alternative to manual feature engineering [13].

B. Stage 2: Conventional Neural Networks for MRI Segmentation:

From Table 4, it is clear that convolutional neural networks (CNNs) have significantly advanced the field of MRI segmentation by enabling automatic extraction of features directly from raw image data [14]. Notable CNN architectures such as AlexNet, VGGNet, and 2D-CNNs have been adapted for medical image analysis tasks [15]. These models typically apply convolutional filters to local image regions, and this allows them to learn spatial hierarchies from the inputs [16].

In MRI segmentation specifically, CNNs have been effectively used for pixel classification through the use of patch-based strategies and shallow grid designs [17]. These strategies help reduce computational cost while still benefiting from spatial information at the correction level.

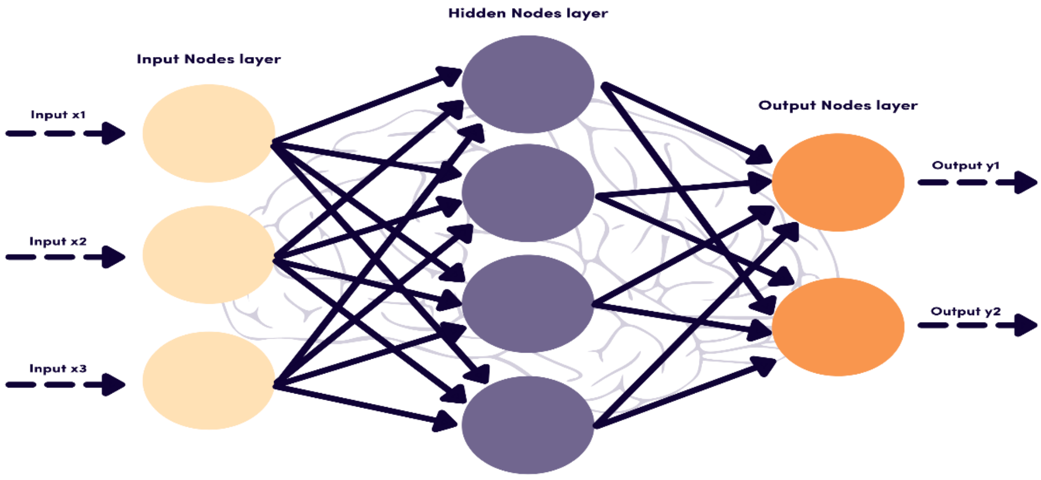

Fig. 2 An example of a conventional neural network

Among the most important positives of CNN networks:

- It has a strong ability to capture hierarchical spatial features [18].
- Removing hand-made features by learning directly from raw pixel data [19].

As for the negatives of early CNN networks:

- Loss of precise spatial resolution due to aggregation and segmentation processes across layers [20].
- Limited reception field in shallow networks, which leads to low context awareness [21].
- Performance deteriorates when applying 2D CNNs to 3D MRI volumes, as spatial dependencies across slices are ignored [22].

As for the solutions that have been explored to address these negatives:

- Using full convolutional networks (FCNs) to maintain spatial dimensions across the network pipeline [23].
- Using 3D CNNs for full volumetric segmentation, this allows spatial continuity across slices [24].
- Introduce extended convolutions to expand received fields without reducing the accuracy of the feature map [25].

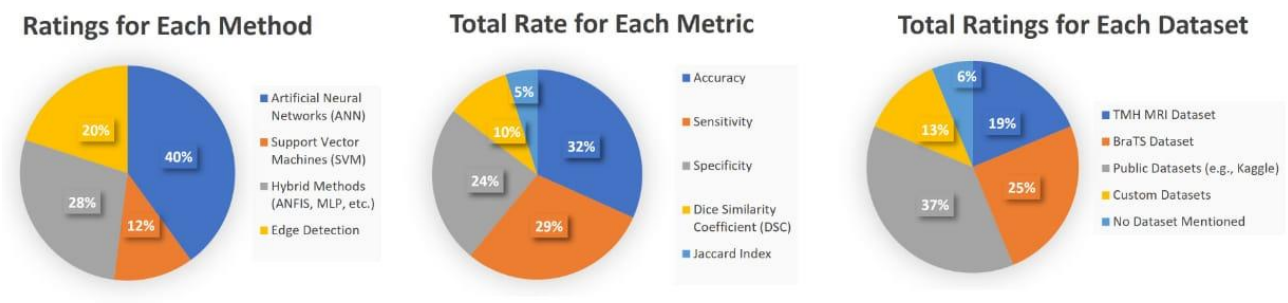

Fig. 3 The ratios of the most important methods, metrics, and datasets used in conventional neural network studies

Fig. 3 shows how the use of methods, metrics, and data sets is distributed during this stage. It highlights the dominance of CNN-based methods, especially 2D CNNs and early volumetric models, as well as performance metrics such as Dice Score and IoU. Datasets such as BraTS, ACDC, and ISIC have been frequently used in evaluating these models.

As for the proposed progress:

The development of U-Net architectures was a breakthrough, combining encryption and decryption designs with skip connections to enhance local and contextual translation performance in segmentation tasks [26].

C. Stage 3: Deep Learning for MRI Segmentation:

From Table 5, note that deep learning architectures have transformed MRI segmentation by introducing encoding and decoding structures capable of capturing hierarchical [27], nonlinear, and multi-scale patterns in medical imaging data. Among the most widely adopted models are U-Net, 3D U-Net, V-Net, and hybrid approaches such as GAN-based segmentation frameworks [28]. These structures take advantage of deep layers to extract features and reconstruct segmentation masks while preserving spatial details [29].

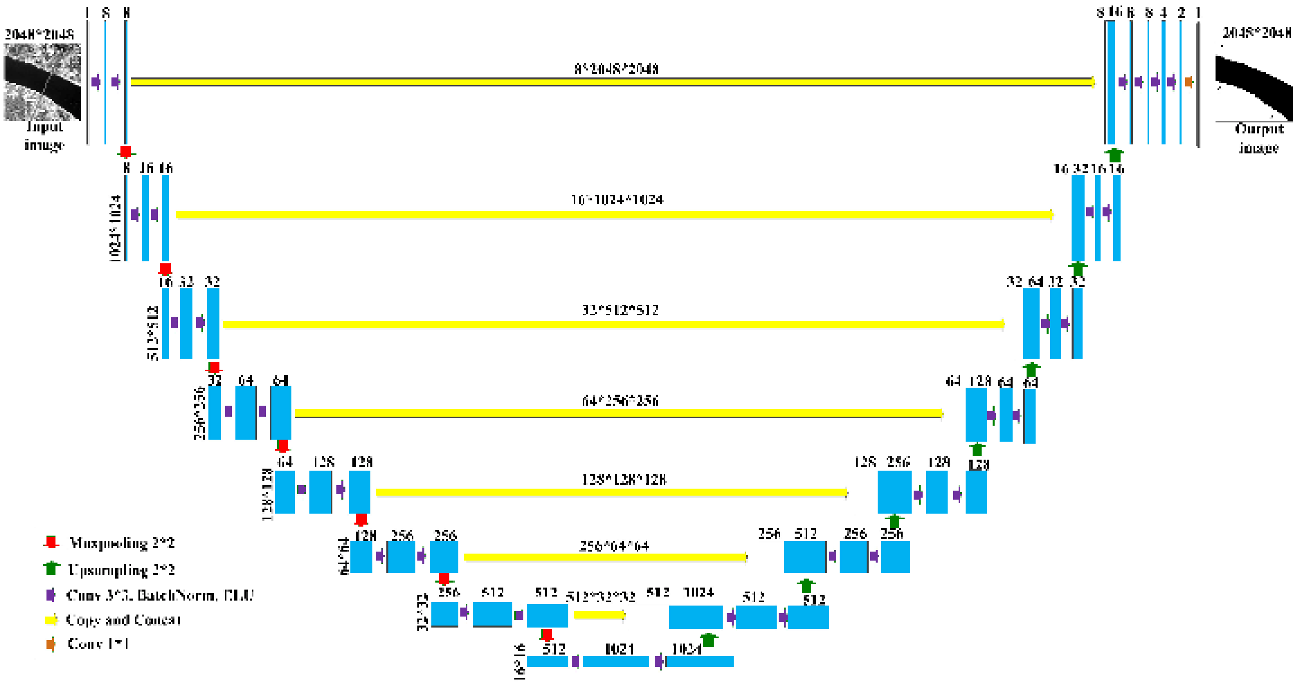

Fig. 4 U-NET Architecture

Among the most important positives of deep learning architectures are:

- Deliver powerful performance through diverse data sets and imaging methods [30].
- Effectively segment complex tissue boundaries and irregular tumor geometry [31].
- Achieve high accuracy in leading benchmark challenges such as BraTS, ACDC and ISIC (refer to Table 1).

The most important negatives include:

- High computational demand and memory usage, especially for volumetric (3D) data [32].
- Ability to over-process when training on limited data [33].
- Inadequate global context modeling in traditional convolutional frameworks [34].

The most important ways to overcome these negatives are:

- Use of data augmentation techniques (for example, rotation, scaling, flipping) to artificially expand the training set and promote generalization of the model [35].
- Designing hybrid models by combining CNNs with advanced modules such as conditional GANs and residual networks, thus improving organization and learning dynamics [36].

• Integrating attention gates (AGs) within the encoding and decoding pipelines to direct the focus of the model to relevant anatomical regions and also improve segmentation accuracy [37].

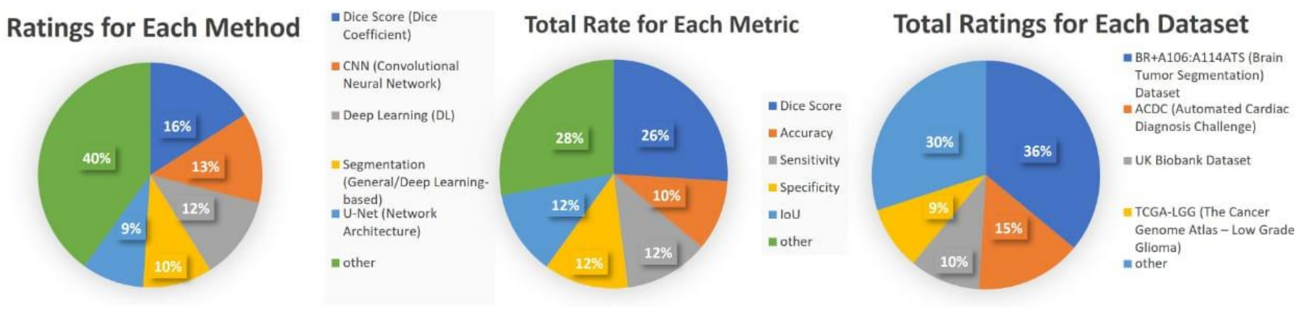

Fig. 5 The ratios of the most important methods, metrics, and datasets used in deep neural network studies.

As shown in Fig. 5, we note that deep learning methods, especially U-Net variants, dominate modern research. Rating metrics such as Dice Score, IoU, and Hausdorff Distance, as well as data sets such as BraTS 2020, ACDC, and ISIC 2017, are frequently used to evaluate model performance and reliability.

As for the proposed progress:

To further improve segmentation quality, U-Net-based architectures can be extended by incorporating attention mechanisms and fuzzy pooling layers [38]. This combination addresses loss of accuracy due to pooling processes and improves contextual awareness by enabling the model to adaptively weigh spatial features based on their importance [39].

D. Stage 4: Attention Mechanisms and Improved Networks for MRI Segmentation:

From Table 6, it is noted that the latest developments in MRI segmentation take advantage of attention mechanisms and transformer architectures to significantly improve model performance[40].These techniques allow models to selectively focus on the most relevant parts of the image, and this improves accuracy in complex medical imaging tasks [41]. Prominent models such as Attention U-Net, TransUNet, AGSE-VNet, and 3D Antice U-Net have shown exceptional segmentation results, especially for difficult tasks such as brain tumor and heart segmentation [42].

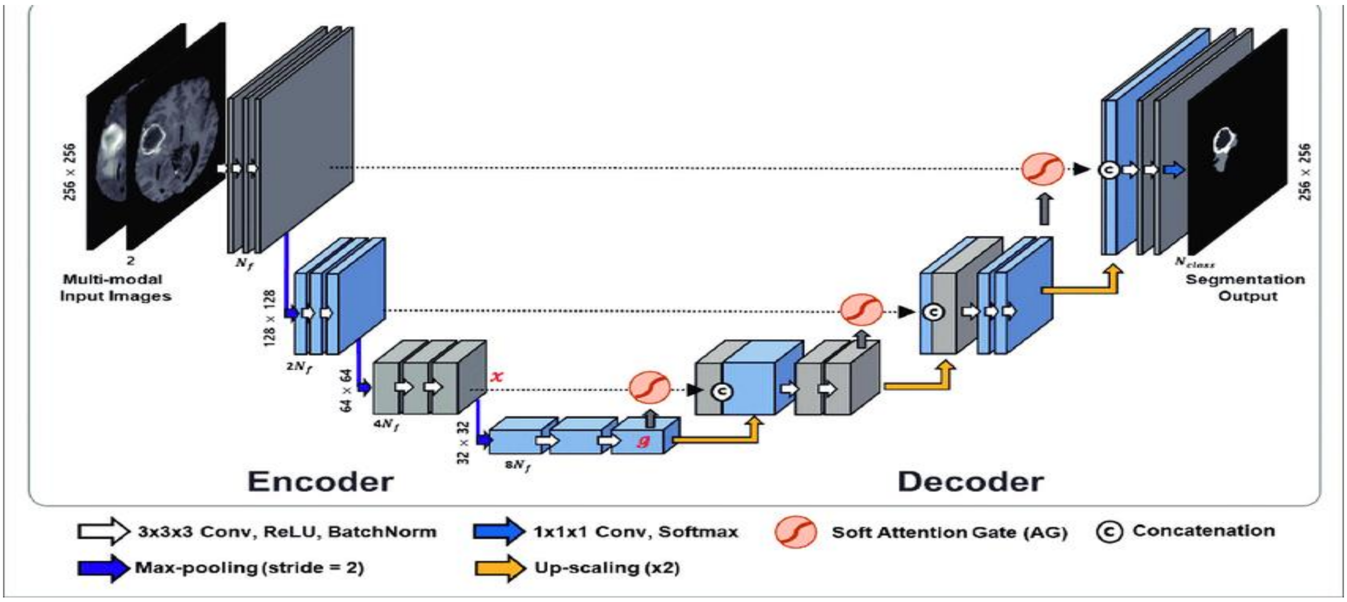

Fig. 6 Architecture of Attention U-net

The most important positives of attention-enhanced models and transformer-based models are:

- Improved localization of complex anatomical structures, such as tumor boundaries or heart tissue [43].
- Ability to model long-term dependencies, especially in large images, where global context is essential for fine-grained segmentation [44].
- Superior performance over well-established public datasets such as BraTS and ACDC (cf.Table 6).

The most important negatives are:

- Increased architectural complexity and longer training times due to the integration of attentional layers and adapters [45].
- Strong reliance on large-scale disaggregated datasets, and this may limit access to smaller or specialized datasets [46].
- Limited generalization to previously invisible imaging areas or different patient groups [47].

As for the most important ways to overcome the negatives, they are:

- Use of pre-trained spine or transfer learning from large natural image datasets (for example, ImageNet) to reduce the need for large-scale medical datasets [48].
- Multimodal imaging (eg, combination MRI, CT, and PET) can improve segmentation power across different imaging conditions [49].
- Use training techniques across datasets and domain adaptation to improve models for better generalization across diverse datasets [50].

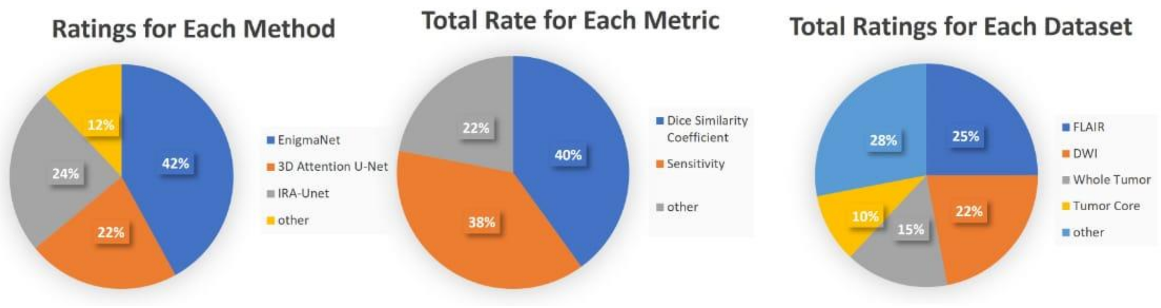

Fig. 7 The ratios of the most important methods, metrics, and datasets used in Attention Mechanisms and Improved Networks studies

As for the proposed progress:

The next step involves the development of an attention-enhanced nested U-Net [51], incorporating fuzzy pooling layers to improve feature selectivity and contextual awareness [52]. This architecture addresses the problems of maximum/average pooling by preserving fine details while improving model performance [53], as shown in the experimental results in Tables 2 and 6.

II. DISCUSSION

This review has explored the evolution of MRI segmentation techniques from traditional machine learning (ML) approaches to deep learning architectures and the recent incorporation of attention mechanisms. Each of the phases has advanced segmentation capabilities in medical imaging, with the combination of these methods improving accuracy and reliability. This section discusses the strengths and limitations of each stage, in addition to proposing potential solutions and highlighting the latest developments.

A. Machine learning methods

Early methods for MRI segmentation were based on traditional machine learning algorithms, including k-NN, SVM, random forests, and others. These methods relied primarily on hand-made features, such as tissue density and texture, which were manually extracted and then used to classify tissue types.

The strengths of these methods include their simplicity of implementation and relatively low computational cost compared to more complex models such as deep neural networks. However, feature engineering represents a critical challenge, as the process is time-consuming and error-prone, especially when dealing with complex anatomical structures [7]. In addition, these models are not well-suited to capturing the spatial dependencies inherent in medical images, and this limits their effectiveness when segmenting very complex structures such as tumors.

Proposed solutions to these challenges include hybrid models that combine image processing techniques (e.g., watershed segmentation) and machine learning classifiers (e.g., SVM). Furthermore, feature selection techniques such as PCA and LDA can enhance the generalizability of these models across diverse datasets, addressing the weak generalization problem [11]. In addition, with the advent of deep learning methods, the manual feature extraction process can be greatly automated, providing greater scalability and accuracy in the long term.

B. Convolutional neural networks (CNNs)

As medical imaging advances, CNNs have emerged as a powerful tool for automating feature extraction directly from raw image data. Where 2D CNNs (for example, AlexNet and VGGNet) have been adapted for medical imaging tasks, this enables better pixel-level classification and tissue segmentation. These networks have shown significant improvement compared to classical machine learning methods, especially concerning learning hierarchical features [15].

Despite their success, CNNs have limitations. Early CNN models often suffer from a loss of spatial resolution due to pooling layers, and the receptive field of 2D CNNs is too limited to fully capture contextual information in larger images, leading to degraded performance in 3D volume segmentation [17]. 3D CNNs provide a solution to these problems by maintaining spatial resolution, but they come at the cost of increased computational requirements [24].

To overcome these challenges, various modifications to CNNs have been proposed, such as introducing full convolutional networks (FCNs) to maintain spatial dimensions during segmentation [23], and using expanding convolutions to expand the receptive field without losing accuracy. In addition, the introduction of U-Net architectures, with skip connections and encoding and decoding frameworks, has helped mitigate problems related to information loss during the sampling process, and this provides better medical image segmentation results.

C. Deep learning architectures

The evolution of deep learning structures has given rise to more complex networks capable of learning nonlinear layouts and adapting to a wide variety of anatomical structures. U-Net, 3D U-Net, V-Net, and hybrid models, such as GAN-based approaches, have become the backbone of modern medical segmentation [28]. These models have significantly improved segmentation performance across different parameters, especially for difficult segmentation tasks such as tumor detection and cardiac segmentation.

The main advantage of these models lies in their ability to handle complex tissue boundaries and irregular shapes, and this provides high accuracy in well-established data sets such as BraTS, ACDC, and ISIC [Table 1]. However, its high computational cost and risk of overfitting small data sets remain a notable concern. 3D models, in particular, suffer from memory and processing limitations, and the lack of understanding of global context in standard CNNs limits their ability to model long-term dependencies [32].

In order to address these problems, solutions such as data augmentation and integration of hybrid models that combine CNNs with GANs or residual networks have been proposed to improve organization and reduce over-processing. In addition, integrating attention gates into encoding and decoding frameworks can help models focus on relevant areas and also improve performance in terms of accuracy and context awareness [37].

D. Attention-enhanced and transformer-based models

The final stage in the development of MRI segmentation focuses on the integration of attention mechanisms and transducers, which has revolutionized image segmentation tasks. Models such as Attention U-Net, TransUNet, AGSE-VNet, and 3D Antice U-Net have shown superior performance on complex tasks such as brain tumor segmentation and cardiac image analysis [52]. These models allow selective focusing on important areas of the image, overcoming the limitations of previous models by capturing long-term dependencies and improving segmentation accuracy, especially for larger or more complex data sets.

While these models offer many advantages, including improved positioning of anatomical boundaries and enhanced modeling of global context, they come with challenges related to architectural complexity and training time [45]. Furthermore, these models require large, labeled datasets to train effectively and often have difficulty generalizing to unseen datasets, especially from different imaging domains.

Solutions to these limitations include the use of pre-trained models and transfer learning from natural image datasets, as well as the integration of multimodal imaging techniques, such as combined MRI, CT, and PET, for more robust segmentation [49]. Training methods across datasets and domain adaptation can also help improve model generalization.

Our proposed advance at this stage is to integrate fuzzy pooling layers into the nested, attention-enhanced U-Net model. This approach addresses the shortcomings of traditional pooling methods by preserving fine detail and improving contextual awareness, providing a promising direction for future research in the field of medical image segmentation.

Finally, advances from machine learning to deep learning, and now to attention-enhanced and transformer-based models, highlight continuing improvements in the accuracy and applicability of MRI segmentation techniques. While significant challenges remain, in particular regarding computational requirements and generalization of models, the development of hybrid models and attention mechanisms holds great promise for the development of medical imaging. By addressing the limitations of previous models and incorporating new techniques such as fuzzy clustering, future segmentation models are likely to achieve higher levels of accuracy, making them more reliable for clinical applications.

III. CONCLUSION

The field of MRI segmentation has seen significant progress over the years, evolving from traditional machine learning methods to sophisticated deep learning and attention enhancement models. Each stage of development has contributed to improved segmentation performance, with notable progress made in dealing with complex medical imaging challenges. This review provided an in-depth exploration of these developments, focusing on four main stages: (1) machine learning methods, (2) convolutional neural networks (CNNs), (3) deep learning structures, and (4) attention-enhanced models.

Although significant progress has been made along the four stages, there are still challenges to overcome. Developing more efficient and scalable models, especially for dealing with large 3D data sets, remains a priority. In addition to all of these, improving the generalizability of the models across different imaging domains and datasets is crucial so as to enhance their clinical applicability. Incorporating multimodal imaging, as well as leveraging translational learning and training across datasets, can help overcome some of these challenges, and this provides more robust and generalizable models. In addition, advances in the possibility of explaining and interpreting deep learning models will increase confidence in these models and their adoption in clinical settings.

REFERENCES

[1] Z. Akkus, A. Galimzianova, A. Hoogi, D. L. Rubin, and B. J. Erickson, “Deep learning for brain MRI segmentation: State of the art and future directions,” J. Digit. Imaging, vol. 30, no. 4, pp. 449–459, 2017, doi: 10.1007/s10278-017-9983-4.
[2] L. Shen, Q. Wang, W. Wang, R. Wang, Y. Yu, and C. Zhang, “Deep attention enhanced networks for medical image segmentation,” Proc. SPIE, vol. 13167, no. RSMIP, p. 126, 2024, doi: 10.1117/12.3029812.
[3] X. X. Yin, L. Sun, Y. Fu, R. Lu, and Y. Zhang, “U-Net-based medical image segmentation,” J. Healthc. Eng., vol. 2022, pp. 1–10, 2022, doi: 10.1155/2022/4189781.
[4] M. Ali, S. O. Gilani, A. Waris, K. Zafar, and M. Jamil, “Brain tumour image segmentation using deep networks,” IEEE Access, vol. 8, pp. 153589–153598, 2020, doi: 10.1109/ACCESS.2020.3018160.
[5] A. Motamedi, “IRA-Unet: Inception residual attention U-Net in adversarial network for cardiac MRI segmentation,” in Proc. ACDC 2017, 2023.
[6] Y. Gu, Z. Piao, and S. J. Yoo, “STHarDNet: Swin transformer with HarDNet for MRI segmentation,” Appl. Sci., vol. 12, no. 1, pp. 1–15, 2022, doi: 10.3390/app12010468.
[7] M. O. Khairandish, M. Sharma, V. Jain, J. M. Chatterjee, and N. Z. Jhanjhi, “A hybrid CNN-SVM threshold segmentation approach for tumor detection and classification of MRI brain images,” IRBM, vol. 43, no. 4, pp. 290–299, 2022, doi: 10.1016/j.irbm.2021.06.003.
[8] H. Peng and S. Yu, “A systematic IoU-related method: Beyond simplified regression for better localization,” IEEE Trans. Image Process., vol. 30, pp. 5032–5044, 2021, doi: 10.1109/TIP.2021.3077144.
[9] L. Anand et al., “Development of machine learning and medical enabled multimodal for segmentation and classification of brain tumor using MRI images,” Comput. Intell. Neurosci., vol. 2022, pp. 1–12, 2022, doi: 10.1155/2022/7797094.
[10] B. Chen, Y. Liu, Z. Zhang, G. Lu, and A. W. K. Kong, “TransAttUnet: Multi-level attention-guided U-Net with transformer for medical image segmentation,” IEEE Trans. Emerg. Top. Comput. Intell., vol. 8, no. 1, pp. 55–68, 2024, doi: 10.1109/TETCI.2023.3309626.
[11] E. J. van Kempen et al., “Accuracy of machine learning algorithms for the classification of molecular features of gliomas on MRI: A systematic literature review and meta-analysis,” Cancers (Basel)., vol. 13, no. 11, pp. 9638–9653, 2021, doi: 10.3390/cancers13112606.
[12] T. Tassew, B. A. Ashamo, and X. Nie, “Multimodal MRI brain tumor segmentation using 3D attention UNet with dense encoder blocks and residual decoder blocks,” Multimed. Tools Appl., pp. 1–28, 2024, doi: 10.1007/s11042-024-18942-1.
[13] M. Miledi and S. Dhouib, “VNS metaheuristic based on thresholding functions for brain MRI segmentation,” Int. J. Appl. Metaheuristic Comput., vol. 12, no. 1, pp. 94–110, 2021, doi: 10.4018/IJAMC.2021010106.
[14] H. Cao et al., “Swin-Unet: UNet-like pure transformer for medical image segmentation,” Lect. Notes Comput. Sci., vol. 13803 LNCS, pp. 205–218, 2023, doi: 10.1007/978-3-031-25066-8_9.
[15] P. A. N. Yi, L. I. U. Jin, T. I. A. N. Xu, L. A. N. Wei, and G. U. O. Rui, “Hippocampal segmentation in brain MRI images using machine learning methods: A survey,” Chinese J. Electron., vol. 30, no. 5, pp. 793–814, 2021, doi: 10.1049/cje.2021.06.002.
[16] M. Z. Alom, C. Yakopcic, M. Hasan, T. M. Taha, and V. K. Asari, “Recurrent residual U-Net for medical image segmentation,” J. Med. Imaging, vol. 6, no. 01, p. 1, 2019, doi: 10.1117/1.JMI.6.1.014006.
[17] G. Xu, X. Zhang, X. He, and X. Wu, “LeViT-UNet: Make faster encoders with transformer for medical image segmentation,” Lect. Notes Comput. Sci., vol. 14432 LNCS, pp. 42–53, 2024, doi: 10.1007/978-981-99-8543-2_4.
[18] H. Wang, P. Cao, J. Yang, and O. Zaiane, “MCA-UNet: Multi-scale cross co-attentional U-Net for automatic medical image segmentation,” Health Inf. Sci. Syst., vol. 11, no. 1, pp. 1–14, 2023, doi: 10.1007/s13755-022-00209-4.
[19] N. Varuna Shree and T. N. R. Kumar, “Identification and classification of brain tumor MRI images with feature extraction using DWT and probabilistic neural network,” Brain Informatics, vol. 5, no. 1, pp. 23–30, 2018, doi: 10.1007/s40708-017-0075-5.
[20] S. Gordon, B. Kodner, T. Goldfryd, M. Sidorov, J. Goldberger, and T. R. Raviv, “An atlas of classifiers—A machine learning paradigm for brain MRI segmentation,” Med. Biol. Eng. Comput., vol. 59, no. 9, pp. 1833–1849, 2021, doi: 10.1007/s11517-021-02414-x.
[21] D. Cheng et al., “Attention based multi-scale nested network for biomedical image segmentation,” Heliyon, vol. 10, no. 14, p. e33892, 2024, doi: 10.1016/j.heliyon.2024.e33892.
[22] Z. Khan, N. Yahya, K. Alsaih, M. I. Al-Hiyali, and F. Meriaudeau, “Recent Automatic Segmentation Algorithms of MRI Prostate Regions: A Review,” IEEE Access, vol. 9, pp. 97878–97905, 2021, doi: 10.1109/ACCESS.2021.3090825.
[23] M. Hamiane and F. Saeed, “SVM classification of MRI brain images for computer-assisted diagnosis,” Int. J. Electr. Comput. Eng., vol. 7, no. 5, pp. 2555–2564, 2017, doi: 10.11591/ijece.v7i1.pp2555-2564.
[24] A. E. Ilesanmi, T. O. Ilesanmi, and B. O. Ajayi, “Reviewing 3D convolutional neural network approaches for medical image segmentation,” Heliyon, vol. 10, no. 6, p. e27398, 2024, doi: 10.1016/j.heliyon.2024.e27398.
[25] A. Magdy, K. N. Ismail, M. H. Mohamed, M. Hassaballah, H. Mahmoud, and M. M. Abdelsamea, “PolyRes-Net: A Polyhierarchical Residual Network for Decoding Anatomical Complexity in Medical Image Segmentation,” IEEE Access, vol. 13, no. Sept. 2024, pp. 15312–15323, 2024, doi: 10.1109/ACCESS.2024.3475877.
[26] J. Chen et al., “TransUNet: Transformers Make Strong Encoders for Medical Image Segmentation,” pp. 1–13, 2021, [Online]. Available: http://arxiv.org/abs/2102.04306

[27] Y. Zhou, Q. Kong, Y. Zhu, and Z. Su, “MCFA-UNet: Multiscale Cascaded Feature Attention U-Net for Liver Segmentation,” IRBM, vol. 44, no. 4, p. 100789, 2023, doi: 10.1016/j.irbm.2023.100789.
[28] M. Jafari and R. Shafaghi, “A Hybrid Approach for Automatic Tumor Detection of Brain MRI Using Support Vector Machine and Genetic Algorithm,” Glob. J. Sci. Eng. Technol., no. 3, pp. 1–8, 2012.
[29] O. Bernard et al., “Deep Learning Techniques for Automatic MRI Cardiac Multi-Structures Segmentation and Diagnosis: Is the Problem Solved?,” IEEE Trans. Med. Imaging, vol. 37, no. 11, pp. 2514–2525, 2018, doi: 10.1109/TMI.2018.2837502.
[30] W. Guo, “Explainable Artificial Intelligence for 6G: Improving Trust between Human and Machine,” IEEE Commun. Mag., vol. 58, no. 6, pp. 39–45, 2020, doi: 10.1109/MCOM.001.2000050.
[31] T. Chithambaram and K. Perumal, “Brain Tumor Detection and Segmentation in MRI Images Using Neural Network,” Int. J. Adv. Res. Comput. Sci. Softw. Eng., vol. 7, no. 3, pp. 155–164, 2017, doi: 10.23956/ijarcsse/v7i3/0164.
[32] D. M. Joshi, N. K. Rana, and V. M. Misra, “Classification of brain cancer using artificial neural network,” in Proc. 2010 2nd Int. Conf. Electron. Comput. Technol. (ICECT), no. June 2010, pp. 112–116, 2010, doi: 10.1109/ICECTECH.2010.5479975.
[33] J. Wu et al., “U-Net combined with multi-scale attention mechanism for liver segmentation in CT images,” BMC Med. Inform. Decis. Mak., vol. 21, no. 1, pp. 1–12, 2021, doi: 10.1186/s12911-021-01649-w.
[34] N. S. Punn and S. Agarwal, Modality specific U-Net variants for biomedical image segmentation: a survey, vol. 55, no. 7. Springer Netherlands, 2022, doi: 10.1007/s10462-022-10152-1.
[35] R. Yousef, G. Gupta, N. Yousef, and M. Khari, A holistic overview of deep learning approach in medical imaging, vol. 28, no. 3. Springer Berlin Heidelberg, 2022, doi: 10.1007/s00530-021-00884-5.
[36] K. K. Hiran and R. Doshi, “An Artificial Neural Network Approach for Brain Tumor Detection Using Digital Image Segmentation,” Int. J. Emerg. Trends Technol. Comput. Sci., vol. 2, no. 5, pp. 227–231, 2013.
[37] M. Sharma, “Brain Tumor Segmentation using hybrid Genetic Algorithm and Artificial Neural Network Fuzzy Inference System (ANFIS),” Int. J. Fuzzy Log. Syst., vol. 2, no. 4, pp. 31–42, 2012, doi: 10.5121/ijfls.2012.2403.
[38] D. A. Shoieb, K. M. Fathalla, S. M. Youssef, and A. Younes, “CAT-Seg: cascaded medical assistive tool integrating residual attention mechanisms and Squeeze-Net for 3D MRI biventricular segmentation,” Phys. Eng. Sci. Med., vol. 47, no. 1, pp. 153–168, 2024, doi: 10.1007/s13246-023-01352-2.
[39] D. Jha, M. A. Riegler, D. Johansen, P. Halvorsen, and H. D. Johansen, “DoubleU-Net: A Deep Convolutional Neural Network for Medical Image Segmentation,” Jun. 2020.
[40] M. H. Guo et al., “Attention mechanisms in computer vision: A survey,” Comput. Vis. Media, vol. 8, no. 3, pp. 331–368, 2022, doi: 10.1007/s41095-022-0271-y.
[41] R. Gu et al., “CA-Net: Comprehensive Attention Convolutional Neural Networks for Explainable Medical Image Segmentation,” IEEE Trans. Med. Imaging, vol. 40, no. 2, pp. 699–711, 2021, doi: 10.1109/TMI.2020.3035253.
[42] J. Liu et al., “Multi-Scale Hybrid Attention Convolutional Neural Network for Automatic Segmentation of Lumbar Vertebrae From MRI,” IEEE Access, vol. 12, no. January, pp. 77999–78013, 2024, doi: 10.1109/ACCESS.2024.3407833.
[43] S. Kuang et al., “MSCDA: Multi-level semantic-guided contrast improves unsupervised domain adaptation for breast MRI segmentation in small datasets,” Neural Networks, vol. 165, pp. 119–134, 2023, doi: 10.1016/j.neunet.2023.05.014.
[44] M. Bonada et al., “Deep Learning for MRI Segmentation and Molecular Subtyping in Glioblastoma: Critical Aspects from an Emerging Field,” Biomedicines, vol. 12, no. 8, 2024, doi: 10.3390/biomedicines12081878.
[45] G. Han et al., “Improved U-Net based insulator image segmentation method based on attention mechanism,” Energy Reports, vol. 7, pp. 210–217, 2021, doi: 10.1016/j.egyr.2021.10.037.
[46] S. R. Gunasekara, H. N. T. K. Kaldera, and M. B. Dissanayake, “A Systematic Approach for MRI Brain Tumor Localization and Segmentation Using Deep Learning and Active Contouring,” J. Healthc. Eng., vol. 2021, 2021, doi: 10.1155/2021/6695108.
[47] A. Al-Saegh, “Identifying a Suitable Signal Processing Technique for MI EEG Data,” Tikrit J. Eng. Sci., vol. 30, no. 3, pp. 140–147, 2023, doi: 10.25130/tjes.30.3.14.
[48] A. Dosovitskiy et al., “An Image Is Worth 16×16 Words: Transformers for Image Recognition At Scale,” ICLR 2021 - 9th Int. Conf. Learn. Represent., 2021.
[49] J. Bleker et al., “A deep learning masked segmentation alternative to manual segmentation in biparametric MRI prostate cancer radiomics,” Eur. Radiol., vol. 32, no. 9, pp. 6526–6535, 2022, doi: 10.1007/s00330-022-08712-8.
[50] T. Chithambaram and K. Perumal, “Edge Detection Algorithms Using Brain Tumor Detection and Segmentation Using Artificial Neural Network Techniques,” Int. Res. J. Adv. Eng. Sci., vol. 1, no. 3, pp. 135–140, 2016.
[51] M. K. Müller et al., “Flexible multi-node simulation of cellular mobile communications: the Vienna 5G System Level Simulator,” EURASIP J. Wirel. Commun. Netw., vol. 2018, no. 1, 2018, doi: 10.1186/s13638-018-1238-7.
[52] X. Guan et al., “3D AGSE-VNet: an automatic brain tumor MRI data segmentation framework,” BMC Med. Imaging, vol. 22, no. 1, pp. 1–18, 2022, doi: 10.1186/s12880-021-00728-8.
[53] H. Ye, R. Zhou, J. Wang, and Z. Huang, “FMAM-Net: Fusion Multi-Scale Attention Mechanism Network for Building Segmentation in Remote Sensing Images,” IEEE Access, vol. 10, no. December, pp. 134241–134251, 2022, doi: 10.1109/ACCESS.2022.3231362.

Table 1. A summary of MRI datasets used in the reviewed studies

No.	Dataset name	Source /Publisher	No. of images	Tumor types	modality	Segmentation tasks	Classification tasks	Reference
1	BraTS (Brain Tumor Segmentation)	MICCAI	2000+	Gliomas (Low-grade, High-grade)	MRI	Tumor segmentation (whole, core, and enhancing tumor)	Tumor classification (benign vs malignant)	[39]
2	ISLES (Ischemic Stroke Lesion)	MICCAI	500+	Ischemic Stroke Lesions	MRI	Stroke lesion segmentation	null	[40]
3	LiTS (Liver Tumor Segmentation)	MICCAI	1316	Liver tumors	CT/MRI	Liver tumor segmentation	null	[27]
4		MICCAI	350+	Gliomas	MRI	Tumor segmentation (whole, core, enhancing)	Tumor grading and type classification	[27]
5	GBM (Glioblastoma Multiforme)	Publicly Available	200+	Glioblastoma	MRI	Tumor segmentation	Tumor classification (grading)	[39]
6	RMI (Retinopathy of Prematurity)	Kaggle	1000+	Retinopathy of Prematurity	Fundus/Optical	Segmentation of Retinal Vessels	Classification (normal vs abnormal)	[27]
7	DCE-MRI (Dynamic Contrast MRI)	Institutional Database	1000+	Various Brain Tumors	MRI (Dynamic)	Tumor segmentation	Tumor classification (benign vs malignant)	[27]
8	DeepBrain (Brain Tumor Dataset)	Kaggle	2000	Glioma, Meningioma, Pituitary	MRI	Brain tumor segmentation	Brain tumor classification	[28]
9	Brain MRI Tumor Dataset	Publicly Available	250	Glioma, Meningioma	MRI	Tumor segmentation	Tumor classification (benign vs malignant)	[29]
10	SYNTH3D (Synthetic MRI Dataset)	Research Lab	1000+	Synthetic tumors	MRI	Synthetic tumor segmentation	null	[41]

Table 2. The use of the dice similarity coefficient (DSC), cross-union (IoU), sensitivity, privacy, and Hausdorff distance at different stages of the MRI process

Phase	**Dice Similarity Coefficient (DSC)**	**Intersection over Union (IoU)**	**Sensitivity**	**Specificity**	**Hausdorff Distance**
Phase 1: Preprocessing	Used to compare the initial preprocessing segmentation with the ground truth	Measures the overlap of preprocessed image regions	Assesses how many true positives are detected in preprocessing	Measures the true negative rate in the preprocessing phase	Assesses the distance of boundary points in preprocessed images
Phase 2: Feature Extraction	Evaluates the feature segmentation accuracy against ground truth	Used to validate feature detection regions	Measures the sensitivity of the extracted features	Evaluates the specificity of the extracted features	Used to check the boundary distance for feature regions
Phase 3: Segmentation	Primary metric to evaluate segmentation accuracy	Used to assess the overlap between predicted segments and ground truth	Quantifies the sensitivity of the segmented structures	Quantifies the specificity of segmented regions	Measures the distance between the boundaries of segmented regions
Phase 4: Postprocessing & Evaluation	Evaluates the refined segmentation accuracy	Validates post-processed segment accuracy	Assesses how well postprocessing detects true positives	Assesses how well postprocessing avoids false positives	Final evaluation of the boundary accuracy after postprocessing

Table 3. Details of the reviewed studies for the machine learning stage

Paper	Reference	Method	Dataset	metric	Result with a number	Calculator and software specifications used by the experiment
Machine learning and deep learning approach for medical image analysis: diagnosis to detection	[1], 2023	ML: SVM, RF, Naive Bayes; DL: ANN, CNN; TL for large datasets; literature review.	The study uses various public and self-created MRI, CT, PET, and X-ray datasets.	Metrics include accuracy, sensitivity, and specificity . The study provides detailed evaluation metrics for ML and DL techniques .	CNN achieved 97.6% accuracy, followed by RF at 96.93%, SVM at 95.05%, DT at 93.35%, LR at 93.01%, and ResNet50V2 at 85.71%.	Experiments were run on a 64-bit computer with an Intel i3 CPU, 8GB RAM, using Python on Google Colab.
Retracted: A Hybrid Approach Based on Deep CNN and Machine Learning Classifiers for the Tumor Segmentation and Classification in Brain MRI	[2], 2023	The paper uses a deep learning algorithm with CNN for tumor segmentation and classification, comparing its methods with previous research and evaluating performance using objective metrics.	The first dataset has 3174 MRI images (2674 tumors, 500 non-tumors), and the second has 3064 images of glioma, meningioma, and pituitary tumors.	The paper defines metrics for evaluating tumor identification, classification, accuracy, segmentation, and image quality, including TP, TN, FP, FN, sensitivity, specificity, DSC, MSE, PSNR, and others.	The study used three brain MRI datasets and evaluated model performance using sensitivity, specificity, accuracy, and the Adam optimizer.	The model was trained for 100 epochs using the Adam optimizer with a learning rate of 0.00001, and evaluated using sensitivity, specificity, and accuracy.
Development of Machine Learning and Medical Enabled Multimodal for Segmentation and Classification of Brain Tumor Using MRI Images	[3], 2022	Geometric mean filter for noise removal, fuzzy c-means for segmentation, GLCM for feature extraction, and SVM, RBF, ANN, and AdaBoost for classification.	One hundred images were randomly selected for the study . 25images contain tumors; 75 are healthy 80 .images were used for training; 20 for testing .Data is available upon request .	Accuracy is a key metric for evaluation . Sensitivity and specificity are also assessed . Various algorithmic approaches are compared for performance.	The SVM RBF algorithm achieved 99% accuracy in classification . 80images were used for training; 20 for testing . 25 out of 100 images contained tumors	The contexts provided do not contain information regarding the calculator and software specifications used in the experiment.
Performance of machine learning algorithms for glioma Segmentation of brain MRI: a	[4], 2021	The study reviews segmentation studies, extracts data, analyzes MLA methods for gliomas, and evaluates performance using DSC scores.	The BraTS dataset was primarily used for segmentation studies . Some studies used original data or TCIA data .	The primary metric used is the DSC score . DSC score ranges from 0.0 to 1.0 . A DSC score of 0.8 indicates good overlap .	Overall DSC score: 0.84 (95% CI: 0.82-0.86) High-grade gliomas DSC score: 0.83 (95% CI: 0.80-0.8)	IBM SPSS Statistics was used for statistical analyses . Version 25.0 of IBM SPSS Statistics was utilized .

Paper	Reference	Method	Dataset	metric	Result with a number	Calculator and software specifications used by the experiment
systematic literature review and meta-analysis				A DSC score of 0.5 indicates poor overlap .	Low-grade gliomas DSC score: 0.82 (95% CI: 0.78-0.87)	Open Meta [Analyst] software was used for quantitative meta-analysis.
VNS Metaheuristic Based on Thresholding Functions for the Brain MRI Segmentation	[5], 2021	The Variable Neighborhood Search (VNS) metaheuristic is used to optimize Otsu's and Kapur's thresholding functions, resulting in VNS-Otsu and VNS-Kapur versions.	Eleven benchmark brain MRI slices are used in the study.	The paper does not specify evaluation metrics.	The paper demonstrates the effectiveness of the VNS-Otsu and VNS-Kapur methods on brain MRI slices.	The contexts provided do not contain information regarding the calculator and software specifications used in the experiment.
Hippocampal Segmentation in Brain MRI Images Using Machine Learning Methods: A Survey	[6], 2021	The text covers traditional, deep learning, atlas-based, label-fusion, classification-based methods, and the U-net framework for segmentation.	HarP :hippocampal segmentation, ABIDE: MRI images, IBSR: manual samples, OASIS: no segmentation, MMMRR: multimodal images, LONI: multi-species MRI.	TP: Correct positives, FP: Incorrect positives, FN: Missed positives, TN: Correct negatives. DSC and JSC: Measure segmentation overlap.	The paper reviews hippocampal segmentation methods, highlighting automated approaches and the use of atlas-based techniques.	The provided contexts do not contain information regarding the calculator and software specifications used in the experiment.
An atlas of classifiers—a machine learning paradigm for brain MRI segmentation	[7], 2021	The text covers AoC for MRI segmentation, compares DC-FCN, nnU-Net, and classifiers for performance.	IBSR18: 18 MRI scans, IBSR20: 20 MRI scans, BrainWeb: 20 simulated images.	Dice scores evaluate performance, p-values assess significance, and mean and standard deviation are reported.	AoC achieved 90.95% for WM, 92.39% for GM, and 76.63% for CSF segmentation on the IBSR18 dataset.	The study utilized the MRBrainS13 dataset for feature extraction . The SPM package was used for data processing
Recent Automatic Segmentation Algorithms of MRI Prostate Regions: A Review	[8], 2021	The text discusses ML and DL techniques, up-sampling, regional proposal, GANs, and model-based hybrid networks for prostate segmentation.	The text lists prostate datasets: PROMISE12, NCI-ISBI 2013, QIN-PROSTATE, I2CVB, PROSTATEx, PROSTATEx-2, and UKM	DSC measures segmentation performance, RVD compares segmented and reference images, and metrics are calculated per slice.	The paper reviews prostate MRI segmentation methods, metrics, datasets, cancer rates, and key research.	The contexts provided do not contain information regarding the calculator and software specifications used in the experiment.
SVM Classification of MRI Brain Images for Computer-	[9], 2017	DWT for noise removal, Canny for edges, Otsu for segmentation,	The dataset contains 40 T2-weighted MRI brain images, with 20 normal and 20 abnormal images	MSE, SNR, and PSNR are used for evaluation.	The SVM classifier achieved 100% accuracy on 40 MRI images. Bior1.3 wavelet denoised with MSE: 6.0511,	MATLAB toolboxes, Canny edge detection, DWT for noise removal, and wavelet

Paper	Reference	Method	Dataset	metric	Result with a number	Calculator and software specifications used by the experiment
Assisted Diagnosis		morphological operations, and SVM with RBF kernel.	featuring various brain diseases.		SNR: 29.2336, PSNR: 40.3124.	types/thresholding were used.
A Machine Learning Approach for MRI Brain Tumor Classification	[10], 2017	Wavelet denoising, median filter, Otsu binarization, K-Means segmentation, and binary tree SVM.	Real-time images from different databases are utilized .Both real-time and simulated images are included .	PSNR measures signal power versus noise power . MSE quantifies differences between predicted and observed values .	The method achieved 96% classification, with eight features, high noise removal, and improved system performance.	The analysis and results were done using MATLAB . Image quality metrics used are PSNR and MSE.
A simple and intelligent approach for brain MRI classification	[11], 2015	Pre-processing for noise and skull removal, feature extraction with color moments, and classification using a neural network.	The study used 70 MRI images: 25 normal and 45 abnormal, divided into training, validation, and testing sets.	Accuracy ,the Similarity index was used for results evaluation . Extra fraction and overlap fraction were also utilized for evaluation .	Training accuracy: 88.9% Validation accuracy: 94.9% Testing accuracy: 94.2% Overall accuracy: 91.8% ANN accuracy: 91.80%	Experiments were conducted on an Intel Core i3 processor (2.40 GHz) with 2 GB of memory, running Windows 7 and MATLAB 7.6.0 (R2008a).
A Hybrid Approach for Automatic Classification of Brain MRI Using Genetic Algorithm and Support Vector Machine	[12], 2010	A hybrid GA-SVM approach with SGLDM feature extraction, 2D wavelet transform, and GA for feature selection.	The study used a dataset of 83 brain MRI images: 29 normal, 22 malignant tumors, and 32 benign tumors.	Sensitivity measures true positives, specificity measures true negatives, and accuracy measures overall classification correctness.	The hybrid approach achieved 94.44%-98.14% accuracy and 91.9%-97.3% sensitivity, excelling in tumor classification.	The contexts provided do not contain information regarding the calculator and software specifications used in the experiment.
Classification of Brain Tumor Type and Grade Using MRI Texture and Shape in a Machine Learning Scheme	[13], 2009	The study uses pattern classification, automated analysis, SVM, and methods like LDA and kNN for tumor classification.	The study involved 98 patients with 102 brain masses, including metastasis, meningiomas, and gliomas.	ACC measures classification correctness, sensitivity shows the true positive rate, specificity shows the true negative rate, and AUC evaluates model performance.	Classification accuracy for metastases vs gliomas: 85%, sensitivity: 87%, specificity: 79%. For high-grade vs low-grade gliomas: accuracy: 88%, sensitivity: 85%, specificity: 96%.	The provided contexts do not contain information regarding the calculator and software specifications used in the experiment

Table 4. Details of the reviewed studies for the conventional neural network stage

Paper	Reference	method	Dataset	metric	Result with a number	Calculator and software specifications used by the experiment
Classification of Brain Cancer using an Artificial Neural Network	[14], 2010	MRI processing uses histogram equalization, segmentation, GLCM for features, and a Neuro Fuzzy Classifier for classification.	Known MRI images from Tata Memorial Hospital (TMH) were used . Unknown MRI samples were also obtained from TMH for testing.	The system classifies MRI images into tumor grades, with results confirmed by cancer specialists from TMH, matching doctors' accuracy.	The system classifies MRI images into Astrocytoma tumor grades .Results show a tumor region extracted from the outer skull.	The provided contexts do not contain information regarding the calculator and software specifications used in the experiment.
Brian Tumor Segmentation using a hybrid Genetic Algorithm and an Artificial Neural Network Fuzzy Inference System (ANFIS)	[15], 2012	MRI processing uses histogram equalization, segmentation, GLCM features, and a Neuro Fuzzy Classifier.	The dataset includes MRI Astrocytoma images, categorized by grade and clustered into four regions: white matter, grey matter, CSF, and tumor.	Sensitivity is one of the evaluation metrics used. Specificity is another important evaluation metric. Accuracy is also measured for performance evaluation.	The method uses ANFIS with 49 fuzzy rules, classifying MRI images from GRADE I to IV, measured by sensitivity, specificity, and accuracy.	MATLAB 7.0.4 is used for feature calculations, with 'histeq' for histogram equalization and GLCM for feature extraction.
Brain Tumor Diagnosis Systems Based on Artificial Neural Networks and Segmentation Using MRI	[16], 2012	Multi-Layer Perceptron (MLP) for classification. Principal Component Analysis (PCA) for feature extraction. WMEM algorithm for image segmentation.	The dataset includes 30 head MRI cases (3 types), 15 gadolinium-enhanced slices per case.	Peak recognition rate is used for evaluation. Average recognition rate is also considered. Norm error measures reconstruction accuracy.	PCA has 100% peak and 78% average recognition, while WMEM has 96.7% peak and 88.2% average.	The contexts provided do not contain information regarding the calculator and software specifications used in the experiment.
Brain Tumor Detection Using Neural Network	[17], 2013	The study uses feature sets, modified Canny, neural networks, and learning vector quantization for tumor classification and detection.	The study uses proton Magnetic Resonance Spectroscopy images. Different datasets yield varying classification accuracy results.	The paper does not specify evaluation metrics.	The classification accuracy varies across different datasets.	The image processing algorithm is based on a modified Canny edge detection algorithm and implemented using MATLAB
Brain Tumor Segmentation	[18], 2013	The study uses GLCM for feature extraction, Genetic Algorithm for	The dataset consists of MRI images of astrocytoma tumors.	Sensitivity is used for evaluating model performance.	The paper compares tumor segmentation methods,	The contexts provided do not contain information regarding the calculator

Paper	Reference	method	Dataset	metric	Result with a number	Calculator and software specifications used by the experiment
Using Genetic Algorithm and Artificial Neural Network Fuzzy Inference System (ANFIS)		selection, ANFIS for segmentation, and compares segmentation techniques.	Images are categorized by tumor grades I to IV. The images were collected from web resources.	Specificity is another key evaluation metric. Accuracy is also considered for assessment.	highlighting ANFIS for Astrocytoma grades I-IV.	and software specifications used in the experiment.
An Artificial Neural Network Approach for Brain Tumor Detection Using Digital Image Segmentation	[19], 2013	The study uses MRI, image enhancement, watershed segmentation, and neural networks for brain tumor detection.	Brain tumor (MRI image)	Similarity index (S) measures segmentation quality, FPVF and FNVF assess misclassification and lost pixels, and the Jaccard index evaluates volume overlap.	A similarity index S of 80 indicates excellent similarity. Higher S, lower FPVF, and FNVF yield better segmentation results.	MATLAB version 7.6.0 was used for algorithm development.
Detection of Tumor in MRI Images Using Artificial Neural Networks	[20], 2014	The method uses neural networks, GLCM features, MLP classification, and thresholding/edge detection for brain tumor detection.	The study used twenty brain MR images. MR images included normal and abnormal brain tissues.	TP: Correctly identified cancer, TN: Correctly identified normal, FP: Incorrect cancer, FN: Incorrect normal.	Twenty MR images were evaluated, with histogram equalization and segmentation improving tumor assessment.	No specific calculator or software specifications are mentioned in the context.
Edge Detection Algorithms Using Brain Tumor Detection and Segmentation Using Artificial Neural Network Techniques	[21], 2016	Canny edge detection, histogram thresholding for segmentation, neural network classification, and feature extraction/selection to improve accuracy.	The study uses real MRI brain images. T1 and T2-weighted MRI images are specifically utilized.	The paper does not specify evaluation metrics.	The algorithm is flexible, efficient, fast, and accurate for tumor detection and segmentation.	The implementation used the Image Processing Toolbox under MATLAB Software. The experiments were conducted on real MRI images.
Classification of tumors and it stages in brain MRI using support vector	[22], 2017	The paper uses region growing, SVM, and ANN for tumor classification, and TKFCM for segmentation.	The dataset includes 39 brain MRI images for normal/tumor classification and 37 images for benign/malignant tumor stage classification.	TP, TN, FP, and FN measure tumor classification; sensitivity is 98%, specificity is 100%, accuracy is 97.37%, and BER is 0.0294.	Sensitivity: 98% Specificity: 100% Accuracy: 97.37% BER: 0.0294	The contexts provided do not contain information regarding the calculator and software specifications used in the experiment.

Paper	Reference	method	Dataset	metric	Result with a number	Calculator and software specifications used by the experiment
machine and artificial neural network						
Brain Tumor Detection and Segmentation in MRI Images Using Neural Network	[23], 2017	The method uses MRI, Canny edge detection, a Gaussian filter, Cellular Automata, and an ANN for brain tumor detection.	The study utilized MRI brain images for analysis. Data was developed from scanning labs and 1.5T scanners.	Accuracy: Correct classifications. Sensitivity: True positives. Specificity: True negatives. TP, TN, FP, FN: Classification outcomes.	The algorithm effectively detects tumors with edge detection, performing better on high-grade tumors across multiple images.	The system was implemented using MATLAB. MATLAB provides powerful mathematical and image processing capabilities.
Fully automatic model-based segmentation and classification approach for MRI brain tumor using artificial neural networks	[24], 2018	The study uses HOG features, neural networks, and supervised learning for segmentation and classification, evaluated against manual methods.	A total of 200 MRI cases were utilized. Digitized medical MR images from standard challenge datasets were used.	SSIM measures image similarity, PRI assesses segmentation accuracy, VoI quantifies information difference, and GCE evaluates segmentation consistency.	Identification precision recorded at 92.14%. Sensitivity achieved was 89%. Specificity reached 94%.	The contexts provided do not contain information regarding the calculator and software specifications used in the experiment.
Identification and classification of brain tumor MRI images with feature extraction using DWT and probabilistic neural network	[25], 2018	The method uses GLCM features, DWT segmentation, morphological filtering, and a probabilistic neural network for tumor detection.	The study used 650 samples from Diacom and radiologists, including 18 infected tumor brain tissues and normal samples.	PSNR evaluates image quality, MSE measures image fidelity, and accuracy indicates the correct tumor classification rate.	Nearly 100% accuracy for the trained dataset. %95accuracy for the tested dataset.	The contexts provided do not contain information regarding the calculator and software specifications used in the experiment.
Hippocampal Segmentation in Brain MRI Images Using Machine Learning Methods: A Survey	[26], 2021	The method uses neural networks, GLCM features, MLP classification, and thresholding/edge detection for tumor detection.	The study used twenty brain MR images. MR images included normal and abnormal brain tissues.	TP: Correct cancer identification, TN: Correct normal identification, FP: Incorrect cancer identification, FN: Missed cancer detection.	Twenty brain MR images were evaluated, with histogram equalization improving image definition and segmentation enhancing tumor assessment.	No specific calculator or software specifications are mentioned in the context.

Table 5. Details of the reviewed studies for the deep learning stage

Paper	reference	Method	dataset	metric	Result with a number	Calculator and software specifications used by the experiment
Deep Learning for Brain MRI Segmentation: State of the Art and Future Directions	[27], 2017	The method uses CNN architectures, label fusion, skull stripping, bias correction, registration, and noise reduction for MR image processing.	The study uses various datasets: BRATS, ISLES, mTOP, MSSEG, NeoBrainS12, and MRBrainS for brain tumor and lesion segmentation.	TPR, PPV, DSC, HD, and ASSD measure segmentation accuracy, overlap, boundary distance, and lesion detection precision.	Sensitivity: 93.3% for the detection of 1p19q status. Specificity: 82.22% for the detection of 1p19q status.	The contexts provided do not contain information regarding the calculator and software specifications used by the experiment.
Deep Generative Model-based Quality Control for Cardiac MRI Segmentation	[28], 2020	A VAE-based generative model is used for quality control, with iterative search and Dice metric evaluation.	UK Biobank dataset: 1,500 subjects' short-axis cardiac images. ACDC dataset: 100 subjects with normal and pathology groups.	The evaluation metric used is the Dice metric. Pearson correlation coefficient (r) is also reported. Mean absolute error (MAE) is calculated for predictions.	The proposed method outperforms CNN and hand-crafted features in both correlation and MAE on ACDC and UK Biobank datasets.	The model, implemented in PyTorch, used the Adam optimizer (learning rate 0.0001), a batch size of 16, and was trained for 100 epochs.
Brain Tumour Image Segmentation Using Deep Networks	[29], 2020	An ensemble of 3D CNN and U-Net with patch-based inference and data augmentation is used for segmentation.	The BraTS 2019 dataset includes 335 glioma patients: 259 high-grade, 76 low-grade, and 125 unknown-grade cases.	Dice scores: 0.750 (enhancing), 0.906 (whole), 0.846 (core), compared with state-of-the-art methods.	Dice scores: 0.750 (enhancing tumour), 0.906 (whole tumour), 0.846 (tumour core).	The provided contexts do not contain information regarding the calculator and software specifications used in the experiment.
Segmentation Loss Odyssey	[30], 2020	The paper categorizes loss functions, explores types, and provides implementations.	The contexts do not specify any datasets used in the study.	The Dice coefficient is a common segmentation metric, while IoU loss optimizes object category segmentation.	The question is not relevant to the research paper's content.	The contexts provided do not contain information regarding the calculator and software specifications used in the experiment.

Paper	reference	Method	dataset	metric	Result with a number	Calculator and software specifications used by the experiment
Brain Tumour Image Segmentation Using Deep Networks	[31], 2020	An ensemble of 3D CNN and U-Net is used for segmentation with patch-based inference and data augmentation.	The study used the BraTS 2019 dataset with 335 glioma patients, including 259 high-grade and 76 low-grade cases.	The Dice scores are 0.750, 0.906, and 0.846 for different tumour regions, with a comparison to state-of-the-art methods.	Dice scores: enhancing tumour 0.750, whole tumour 0.906, tumour core 0.846, with patient-specific scores of 0.930, 0.949, and 0.927.	The contexts provided do not contain information regarding the calculator and software specifications used in the experiment.
A Systematic Approach for MRI Brain Tumor Localization and Segmentation Using Deep Learning and Active Contouring	[32], 2021	CNN is used for classification, Faster R-CNN for tumor localization, and Chan-Vese for tumor segmentation.	The study used a T1-weighted MRI brain tumor dataset with 233 patients and 3064 images, focusing on meningioma and glioma, excluding pituitary tumor images.	Dice Score, Rand Index, VOI, GCE, BDE, PSNR, and MAE assess similarity, accuracy, consistency, boundary, quality, and error.	Average Dice Score: 0.92 Accuracy: 94.27% for glioma Cohen's kappa: 0.843 (training), 0.872 (testing(AUC values: 0.93 (training), 0.94 (testing	The contexts provided do not contain information regarding the calculator and software specifications used in the experiment.
AHybrid CNN-SVM Threshold Segmentation Approach for Tumor Detection and Classification of MRI Brain Images	[33], 2021	A hybrid CNN-SVM model for tumor detection uses the BRATS 2015 dataset, with CNN for feature extraction and SVM for classification.	The dataset used is from BRATS 2015. It includes 110 training cases and 220 testing cases.	Accuracy, True Positive Value, and texture features assess image classification and properties.	The hybrid CNN-SVM model achieved 98.4959% accuracy. SVM accuracy was 72.5536%. CNN accuracy was 97.4394%.	The model was implemented on a Dell laptop with a Core i7cpu,8GB RAM, and 4GB Nvidia GPU.
Znet: Deep Learning Approach for 2D MRI Brain Tumor Segmentation	[34], 2022	DNNs for tumor segmentation, using data augmentation, encoders, and trained on TCGA-LGG for 200 epochs.	The study used the TCGA-LGG dataset with 3,929 FLAIR MRI slices, 1,373 labeled abnormalities, annotated by experts.	Pixel accuracy can be misleading; better metrics include IoU, Dice coefficient, F1 score, and MCC for evaluation.	Validation Dice coefficient: 0.96 (training), 0.92 (testing); Pixel accuracy: 0.996; F1 score: 0.81; MCC: 0.81.	The model used 2x Titan GPUs, ADAM optimizer, 128x128 images, and Albumentations for augmentation.
A holistic overview of the deep learning approach in medical imaging	[35], 2022	DL for medical image analysis includes segmentation, classification, augmentation, feature extraction (GLCM/LBP), and PCA.	Public datasets from GitHub and Kaggle are used, with medical image datasets being smaller.	F-beta, ROC, Dice, accuracy, sensitivity, and Jaccard assess performance in segmentation and classification.	0.869 Dice similarity coefficient score achieved in prostate image segmentation	The contexts provided do not contain information regarding the calculator and software specifications used by the experiment.
A deep learning masked segmentation alternative to manual	[36], 2022	DLM VOI segmentation is compared with expert manual segmentation,	The study used a multicenter dataset of 930 patients.	AUC compared DLM and manual segmentation, with sensitivity and specificity	DLM method AUC: 0.76 (95% CI: 0.66-0.85(	Training used TensorFlow Keras 2.2.0 with a 3D U-Net architecture, 32-GB

Paper	reference	Method	dataset	metric	Result with a number	Calculator and software specifications used by the experiment
segmentation in biparametric MRI prostate cancer radiomics		using ROC analysis for performance and iMRMC for model comparison.	Data was collected from 9 different medical centers. Included 2 tertiary care academic institutions and 7 non-academic institutions.	evaluated for the best model.	Manual segmentation AUC: 0.62 (95% CI: 0.52-0.73(Time reduction: over 97% compared to manual segmentation	V100 GPU, Adam optimizer (learning rate 1e-4), batch size of 1, and up to 400 epochs.
A survey of methods for brain tumor segmentation-based MRI images	[37], 2023	Segmentation methods: conventional, supervised, unsupervised, CNN-based, hybrid, and FCM clustering.	The study uses BraTS 2013, 2018, 2019, and 2020 datasets.	Evaluation metrics include accuracy, sensitivity, and specificity for assessing segmentation performance.	Accuracy: Havaei 0.88, Hussain 0.80, Pereira 0.85, Ranjbarzadeh 0.92, Wang 0.90.	The contexts do not include details on the calculator and software specifications used.
Study and analysis of different segmentation methods for brain tumor MRI application	[38], 2023	Otsu's method, Watershed, Level set, K-means, HAAR DWT, and CNN are used for image segmentation and analysis.	The study used the BRATS dataset-2018 for simulations.	Recall, precision, F-measure, and accuracy assess model performance.	Otsu: 71.42%, Watershed: 78.26%, Level set: 80.45%, K-means: 84.34%, DWT: 86.95%, CNN: 91.39% accuracy, CNN response time: 2.519s.	MATLAB was used to simulate segmentation algorithms on the BRATS 2018 dataset, with a CNN response time of 2.519 seconds.
Deep Learning for MRI Segmentation and Molecular Subtyping in Glioblastoma: Critical Aspects from an Emerging Field	[39], 2024	DL for MRI segmentation, ML for tumor classification, Grad-CAM for interpretability, STAPLE for averaging, and data selection for training.	The BraTS and TCIA datasets are used for training DL algorithms, with multi-institutional databases proposed for future research.	AI segmentation is evaluated using Dice Score, Hausdorff distance, and annotation averaging to reduce human error.	Mean patients: 148.6, median: 60.5; 1p19q codeletion prediction accuracy: 92%, algorithms >80-90% accuracy.	The contexts provided do not contain information regarding the calculator and software specifications used in the experiment

Table 6. Details of the reviewed studies for the attention and enhanced networks stage

Paper	Reference	method	Dataset	metric	Result with a number	Calculator and software specifications used by the experiment
EnigmaNet: A Novel Attention-Enhanced Segmentation Framework for Ischemic Stroke Lesion Detection in Brain MRI	[40], 2024	EnigmaNet uses a modified loss function, DWI/FLAIR MRI, Genesis-k blocks, and dual-headed attention for lesion detection.	The study used the ISLES-2015 public dataset. It includes 64 sub-acute ischemic stroke cases. MRI sequences were skull-stripped and co-registered. The dataset is divided into training and testing cases.	Dice score, sensitivity, specificity, accuracy, and AUC-ROC assess segmentation and classifier performance.	EnigmaNet achieved a Dice score of 0.8965 (FLAIR), sensitivity 0.8776, specificity 0.9866; a Dice score of 0.8423 (DWI), sensitivity 0.8452, specificity 0.9754.	The provided contexts do not contain information regarding the calculator and software specifications used in the experiment.
Deep attention-enhanced networks for medical image segmentation	[41], 2024	A deep attention network for segmentation uses DCSegHead, attention decoder, CNN-Swin pyramids, and feature fusion.	The Synapse dataset from the MICCAI 2015 challenge. The ACDC dataset from 100 MRI patients	The primary evaluation metric used is the DSC metric. The method achieved a DSC performance of 90.73.	The model increased the Dice score by 2.26, with a highest score of 10.90 in HD, and an average performance of 90.73 on the DSC metric.	The model was trained in PyTorch on a Tesla T4 GPU with SGD, 224x224 images, batch size 8, and 400 epochs.
Multimodal MRI Brain Tumor Segmentation using 3D Attention UNet with Dense Encoder Blocks and Residual Decoder Blocks	[42], 2023	The 3D Attention U-Net uses dense encoders, residual decoders, attention layers, and BCE-Dice loss, trained on BraTS 2020.	The BraTS 2020 dataset includes 3D MRI scans from 369 patients with gliomas (LGG and HGG), manually annotated by neuroradiologists.	The IoU is the Jaccard Index, and the Dice coefficient is the Dice-Sorensen coefficient, measuring discrepancies between segmentation and ground truth.	Dice scores: WT = 0.889, TC = 0.866, ET = 0.828. Jaccard means not specified.	The model was implemented in Python with PyTorch, trained for 100 epochs using the Lion optimizer and a weight decay of 0.01.
IRA-Unet: Inception Residual Attention Unet in Adversarial Network for	[43], 2023	A deep learning method for cardiac MRI uses IRA-Unet with GAN, attention, and a discriminator for improved segmentation.	The ACDC 2017 dataset has 100 training and 50 test subjects, while the MM challenge dataset includes 375 patients from three countries.	Dice similarity coefficient (DSC), Jaccard similarity index (JC), and Hausdorff distance (HD) are used for performance evaluation.	Mean Dice score for left ventricle: 0.947. Mean Dice score for right ventricle: 0.919. Mean Dice score for myocardium: 0.907.	The contexts provided do not contain information regarding the calculator and software specifications used in the experiments.

Paper	Reference	method	Dataset	metric	Result with a number	Calculator and software specifications used by the experiment
Cardiac MRI Segmentation						
Attention Gate ResU-Net for Automatic MRI Brain Tumor Segmentation	[44], 2020	AGResU-Net uses Attention Gates, DSC, Hausdorff distance, z-score normalization, and Gaussian regularization.	BraTS 2017 dataset with 285 glioma patients. BraTS 2018 dataset for model evaluation. BraTS 2019 dataset for additional experiments	DSC measures overlap, Hausdorff distance estimates surface distance, and Hausdorff95 measures the 95th quantile.	AGU-Net and AGResU-Net outperform U-Net and ResU-Net in tumor segmentation, with attention gates boosting core tumor accuracy.	Models were implemented in Keras with TensorFlow, using an SGD optimizer, PReLU activation, and executed on a PC with a GeForce GTX 1080 GPU.
Automatic segmentation of brain MRI using a novel patch-wise U-net deep architecture	[45], 2020	The paper proposes a patch-wise U-Net for improved segmentation, compared to the U-Net and SegNet.	The OASIS dataset was used for experiments. The Internet Brain Segmentation Repository (IBSR) dataset was also utilized.	The evaluation metrics include Dice similarity coefficient (DSC), Jaccard index (JI), Hausdorff distance (HD), and mean squared error (MSE).	The proposed method achieved a Dice similarity coefficient of 0.93, outperforming U-Net by 3% and SegNet by over 10%.	The model was trained with SGD, momentum 0.99, learning rate 0.001, and categorical cross-entropy loss, using Keras for experiments.
MSCDA: Multi-level semantic-guided contrast improves unsupervised domain adaptation for breast MRI segmentation in small datasets	[46], 2023	The MSCDA framework uses contrastive learning and cross-domain sampling for breast MRI segmentation.	Dataset 1: 11 healthy female volunteers' MRI images and masks. Dataset 2: 134 patients with invasive breast cancer MRI images and masks.	The main evaluation metric is DSC, with auxiliary metrics including JSC, precision, and sensitivity.	MSCDA achieved stable performance with DSC 89.2, outperforming other methods with fewer source subjects.	No information on calculator specifications is provided. No information on software specifications is provided.
Deep learning-based segmentation of brain tissue from diffusion MRI	[47], 2021	DDSeg uses CNN for diffusion MRI segmentation, integrating DKI parameters and comparing with other methods.	The study uses MRI data from multiple sources: HCP, CAP, VERIO, MultiCenter, and SUDMEX.	Accuracy is measured across the brain, for tissue boundaries, and non-boundary regions, with PSI for WM, GM, and CSF.	CNN AT achieved 90.48% accuracy on HCP data and 80.30% on VERIO data. Dice scores indicate prediction accuracy.	The provided contexts do not contain information regarding the calculator and software specifications used in the experiments.
STHarDNet: Swin Transformer with HarDNet for	[48], 2022	The study proposes the STHarDNet model structure.	The study used the ATLAS dataset for MRI segmentation.	Dice measures similarity between predicted and actual values.	STHarDNet achieved a Dice value of 0.5547. STHarDNet achieved IoU value of 0.4185.	Operating System: Windows 10 CPU: Intel Core i9-9900KF 3.6GHz

Paper	Reference	method	Dataset	metric	Result with a number	Calculator and software specifications used by the experiment
MRI Segmentation		It combines HarDNet with Swin Transformer for MRI segmentation. Four performance metrics are used: Dice, IoU, precision, and recall. The ATLAS dataset is utilized for model evaluation	The ATLAS dataset includes 189 MRI scan images. It consists of 43,281 annotated slices. Data from 177 patients were utilized. 80 images were used for training, 52 for validation.	IoU refers to the intersection over union area ratio. Precision indicates the percentage of accurately predicted pixels. Recall measures the model's detection of ground truths.	STHarDNet achieved a precision value of 0.6764. STHarDNet achieved a recall value of 0.5286.	GPU: NVIDIA GeForce RTX 2080Ti RAM: 112GB Storage: 1TB SSD Language: Python 3.7 Framework: PyTorch 1.5
3D AGSE-VNet: an automatic brain tumor MRI data segmentation framework	[49], 2022	AGSE-VNet uses SE for feature enhancement, AG for noise suppression, skip connections, and multi-modal MRI images for segmentation.	The study uses the BraTS 2020 dataset with 369 training and 125 validation cases of LGG and HGG, featuring T1, T1-CE, T2, and FLAIR images.	Dice measures accuracy, specificity, true negatives, sensitivity, true positives, and Hausdorff95 boundary distance.	Dice: 0.68-0.85. Sensitivity: 0.83. Specificity: 0.99. Hausdorff95: 8.96.	The experiment used TensorFlow 1.13.1, Intel Core i7-9750H CPU, 32GB RAM, Nvidia GeForce RTX 2080 GPU, Windows 10, PyCharm, and Python 3.6.9.
Improved U-Net-based insulator image segmentation method based on attention mechanism	[50], 2021	Improved U-Net with ECA-Net attention for insulator segmentation, evaluated using Precision, Recall, and IoU.	The study uses 3000 UAV aerial images from the 8th Teddy Cup, with insulator labels, enhanced through image processing techniques.	Precision, recall, IoU, and F-Score assess prediction accuracy and overlap.	The average overlap IoU of the proposed method is 96.8%. Precision reached 98.35, and Recall reached 98.38. F Score increased to 98.36	The provided contexts do not contain information regarding the calculator and software specifications used in the experiment
Retracted: Brain Tumor Detection and Classification by MRI Using Biologically Inspired Orthogonal Wavelet Transform and	[51], 2023	Tumor segmentation, feature extraction, genetic algorithm, and classification with SVM, Naive Bayes, and CNN.	The dataset includes MRI brain images from 66 patients: 22 normal and 44 abnormal, with T2-weighted 256x256 pixel images.	Jaccard, Dice: measure similarity; sensitivity, specificity: assess classification; accuracy: overall correctness.	The accuracy and confusion matrix results are shown in Figures 15 and 16	MATLAB software was used for the proposed strategy. The system had a Core 2 Duo code configuration.

Paper	Reference	method	Dataset	metric	Result with a number	Calculator and software specifications used by the experiment
Deep Learning Techniques						
Linear Attention Mechanism: An Efficient Attention for Semantic Segmentation	[52], 2021	The paper proposes a linear attention mechanism using a first-order Taylor expansion to reduce memory and computational costs.	The Fine Gaofen Image Dataset (GID) has 10 RGB images, 15 classes, and is split into 7280 patches for training, validation, and testing.	Evaluation uses OA, AA, Kappa, mIoU, and F1-score.	Evaluation metrics: OA, AA, Kappa, mIoU, F1-score. The search does not contain numerical results.	Experiments on RTX 2080ti GPU with PyTorch, Adam optimizer, batch size 16, and cross-entropy loss.
TransAttUnet: Multi-level Attention-guided U-Net with Transformer for Medical Image Segmentation	[53], 2022	TransAttUnet uses multi-level attention, skip connections, and a unified loss function for segmentation.	Datasets used: ISIC-2018, JSRT, Montgomery, 1NIH, Clean-CC-CCII, Data Science Bowl, GlaS.	Metrics used: DICE for similarity, IoU for segmentation accuracy, ACC for overall correctness, REC for true positives, PRE for true vs. predicted positives.	TransAttUnet achieved an IoU score of 84.98. Improvement of 0.91 over previous models. Highest score on almost all evaluation metrics	The contexts provided do not contain information regarding the calculator and software specifications used in the experiments.